Vietnam Journal of Chemistry, International Edition, **55**(6): 781-786, 2017
DOI: 10.15625/2525-2321.2017-00544

Synthesis, characterization and corrosion inhibitive ability of composites silica – polypyrrole

Vu Thi Hai Van[1,3], Pham Thi Nam[1], Nguyen Thi Thom[1], Nguyen Thu Phuong[1], To Thi Xuan Hang[1], Dinh Thi Mai Thanh[2,3*]

[1]*Institute for Tropical Technology, Vietnam Academy of Science and Technology (VAST)*

[2]*University of Science and Technology of Hanoi, VAST*

[3]*Graduate University of Science and Technology, VAST*

Received 22 March 2017; Accepted for publication 25 December 2017

Abstract

Composites silica/polypyrrole (SiO_2/PPy) were synthesized by in-situ, using $FeCl_3$ as oxidant, the quantity of silica is varied from 0.15 g, 0.3 g, 0.45 g to 0.6 g (SP1, SP2, SP3 and SP4, respectively). The morphologies and characterizations of composites were evaluated by FT-IR, EDX, SEM, TEM and TGA. EDX result indicated that the percentage of silicon increase from 20.48 to 28.14 % when the quantities of silica in initial mixture increase. Carbon steel were coated with polyninylbutyral (PVB) resin and PVB coatings containing 10 % SP1, SP2, SP3 and SP4 by spin coating technique. Corrosion protection performance of PVB coating containing SiO_2/PPy was evaluated by measurement of OCP and potentiodynamic polarization. The results shows that the SiO_2/PPy in PVB coating has corrosion inhibitive ability for carbon steel, it can shift the potential of steel into anode areas and reduce the corrosion current density more than 100 times.

Keywords. Composite silica-polypyrrrole, corrosion inhibitive ability, corrosion performance.

1. INTRODUCTION

Corrosion of metals is an enormous problem throughout the world. The bad performance and environmental toxicity of conventional coatings persuade scientists to find a proper replacement coating to combat corrosion [1, 2]. Several techniques have been used to protect metals from corrosion. Polymer coatings maybe are the most widely used technique [3, 4]. Conducting polymers are an important class of polymers which are mainly considered as one of the main components for corrosion-resistant coatings [5]. In general, good corrosion protection requires that the coatings have good adhesion to the metal substrates [6, 7]. Corrosion protection applying conductive polymers was first proposed by MacDiarmid in 1985 [8]. Among these polymers, polypyrrole has been widely studied due to its ease of synthesis, high conductivity and environmental stability [9, 10]. Recently, polypyrrole is reported as a suitable material for corrosion protection purpose.

However, PPy in bulk form is infusible and intractable in nature, insoluble in common solvents [10]. So that many researchers have been focused on the preparation of composite of PPy with metal oxide as Fe_3O_4, TiO_2, ZnO, SiO_2, which are the substrates for the chemical polymerization of polypyrrole [11-14]. Nano silica has been studied for preparation of SiO_2/PPy composites due to its low cost, high surface area and easy dispersion [15, 16].

Hematite-silica-polypyrrole ellipsoidal sandwich composite spheres as well as SiO_2, SiO_2/PPy, PPy hollow capsules and PPy ellipsoidal hollow capsules with movable hematite cores were successfully fabricated by hematite (a-Fe_2O_3) [17]. Armes et al. prepared and characterized of silica–polypyrrole nanocomposite colloids. In this approach, the silica particles acted as a colloidal substrate with high surface for the precipitation of polypyrrole [18, 19]. Perruchot et al., pre-treated of silica gel (in micro size) with organo-silane in order to enhance the conductivity of silica gel–PPy composites [20, 21]. Composites SiO_2/PPy synthesized in aqueous ethanolic solution have nanowire-like structure and particulate-like nanostructured, respectively [22]. Cheng et al. [23] produced mesoporous material with conducting polypyrrole confined in mesoporous silica through adsorption of pyrrole gas and

subsequent oxidative polymerization. Others used steric agents, stabilizers and organo-functionalization to improve the conductivity of composites SiO_2/PPy. In most cases, the particle sizes of the silica used were in the range of 60–500 nm [16, 24].

In this work, we prepared PPy – SiO_2 composites by *in - situ* chemical oxidative polymerization of different concentrations of silica. The nanostructure, composition and corrosion protection performance of the composites were also evaluated.

2. EXPERIMENT

2.1. Chemicals

Pyrrole monomers (97 %, Merck) were distilled under reduced pressure before use. Tetraethyl orthosilicate (TEOS) (98.5 %; Daejung, Korea), Polyvinylbutyral (PVB) (Japan). Hydrogen chloride (38 %; HCl), iron (III) chloride hexahydrate ($FeCl_3.6H_2O$) (99 %), acetone (C_3H_7O) (99.5 %) and methanol (CH_4O) (99.5 %) were purchased from Huakang, China.

2.2. Preparation of silica nanoparticles

TEOS was dropped slowly into HCl solution (pH = 1). The mixture was stirred under magnetic for 24 hours at room temperature then heated 80 ^oC for 24 hours. The precipitate was washed and filtered by distilled water to pH = 7. Finally, the samples were dried at 80 ^oC for 24 h in vacuum oven.

2.3. Preparation of SiO_2/PPy

0.15 g (SP1), 0.3 g (SP2), 0.45 g (SP3), 0.6 g (SP4) of SiO_2 was dispersed in 50 mL H_2O. After sonication for 20 minutes, 25 ml aqueous solution containing 3.57 g $FeCl_3$ was added into the suspension. Then 0.15 g of pyrrole monomer (was dispersed in 25 mL H_2O) was dropped slowly into solution 1. The suspension color turned from yellow to dark green; at last it became black. The reaction mixture was kept stirring for 24 hours to form SiO_2/PPy composites. Finally, the precipitate was washed, filtered by distilled water and the mixture of methanol and acetone 5 times, dried at 80 ^oC for 24 hours.

2.4. Preparation of PVB coating

Carbon steel sheets (40 mm × 60 mm × 2 mm) were used as substrate. The sheets were polished with abrasive paper from 80 to 600 grades and leaned with ethanol. 10 %wt. composites SiO_2/PPy was incorporated in PVB. SiO_2/PPy were dispersed into PVB solution by magnetic stirring, the sonication, the liquid paint was applied by dropping method and dried at ambient temperature for 5 days. The dry film thickness was 18±2 µm (measured by Minitest 600 Erichen digital meter).

2.5. Analytical characterizations

The morphology and compound of the composites were investigated using scanning electron microscope (SEMSM-6510LV) coupled with energy dispersive X-ray spectrometer (EDX) and transmission electron microscopy (TEM) using JEM 1010 transmission electron microscopy operating at 80 kV.

Thermo gravimetric analysis (TGA) was performed using a (TGA209F1) with a heating rate of 10 ^oC per minute in atmosphere.

Fourier transform infrared Spectroscopy (FTIR, Thermal IS10) were recorded in the spectral range of 4000-400 cm^{-1} to analyze the chemical structure of the composite.

2.6. Electrochemical measurement

Three electrodes cell system was used to perform the measurements (Autolab). Open circuit potential (OCP) versus time was employed for electrochemical characterization of the coatings. Three electrodes-cell system was used to perform the measurements (Biologic SAS): the working electrode was steel coated with PVB coatings and PVB coatings containing SP1, SP2, SP3 and SP4 (11 cm^2); Platin was used as counter electrode and SCE was used as reference electrode. The test specimens were kept in the 3 % NaCl solution under open circuit potential conditions for 48 hours, prior to the electrochemical tests.

The polarization curves were obtained starting from the open circuit potential and varying in the range ± 200 mV, with a scan rate of 5 mV/s. The values of corrosion potential (E_{corr}), corrosion current density (i_{corr}), anodic and cathodic Tafel constants (β_a, β_c) obtained by the extrapolation of the linear portions of Tafel plots. The polarization resistance (Rp) values were calculated by using the Stern–Geary equation (1) [25].

$$R_p = \frac{1}{i_{corr}} \times \frac{\beta_a \times \beta_c}{2.303\,(\beta_a + \beta_c)} \quad (1)$$

3. RESULTS AND DISCUSSION

3.1. FTIR analysis

Figure 1 presents the infrared spectra of SiO_2, PPy, SiO_2/PPy synthesized with different quantity of SiO_2. The spectrum of silica shows absorption bands at 3400 cm^{-1} characteristic of –OH group and peaks at 1080 and 470 cm^{-1}characteristic of Si-O-Si antisymmetric and symmetric stretching vibration [26-28].

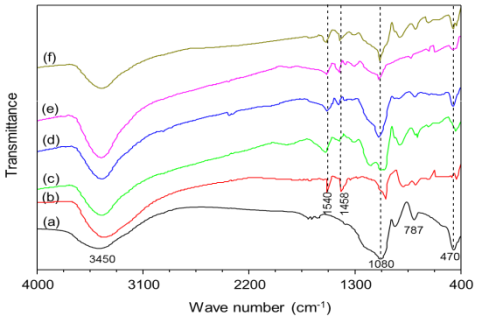

Figure 1: FT-IR spectra of SiO_2 (a), PPy (b), SP1 (c), SP2 (d), SP3 (e) and SP4 (f)

The spectrum of PPy shows the characteristic bands attributable to the C–H in-plane deformation vibration at 1069 cm^{-1}, C–N asymmetric stretching vibration at 1458 cm^{-1}, ring-stretching mode of C-C in Py ring at 1540 cm^{-1} [29], the peak occurring around 3572- 3392 cm^{-1}, correspond to the N-H stretch of the pyrrole ring and maybe stretching vibrations of adsorbed water [30].

Table 1: Wave number for the functional groups of SiO_2 and PPy in composites

Samples	$\upsilon_{Si-O-Si}$	υ_{C-C}	υ_{C-N}
SP1	1080	1545	1460
SP2	1082	1541	1463
SP3	1085	1541	1462
SP4	1082	1542	1460

As seen in table 1, by comparison with the spectra of pure PPy and SiO_2, the characteristic bands of Si-O-Si, C-N and C-C in PPy/SiO_2 have slightly changed. The absorption band which is associated with C-C stretching vibration at 1540 cm^{-1} and the peak at 1458 cm^{-1} represents C-N stretching vibrations changes to higher wave number. In addition, the peak at 1080, 1082, 1085 and 1082 in SP1, SP2, SP3 and SP4, respectively is assigned to the in-plane deformation vibrations of NH_2^+ formed on the polypyrrole chains by protonation, which is overlapped by the peak of the antisymmetric Si-O-Si stretching vibrations of SiO_2, thus, the FTIR spectra of the composite confirm the incorporation of PPy and SiO_2.

3.2. SEM, TEM and EDX of composites

The SEM photographs of pure silica, SP1, SP2, SP3 and SP4 are shown in figure 2. The results show that all the samples have the same shapes, spherical. With pure silica, the diameters are about 50-100 nm, but with the presence of PPy, the diameters of composites increase to 60-200 nm. The morphologies of SP1, SP2, SP3 and SP4 were indicated clearly by TEM (figure 3). In addition, the results show that the higher quantities of silica, the higher diameter of composites. It can be explained that the SiO_2 core is encapsulated by PPy shell, so the diameter of composites increase. The quantity of silica increases, silica overlap each other so making the higher diameter.

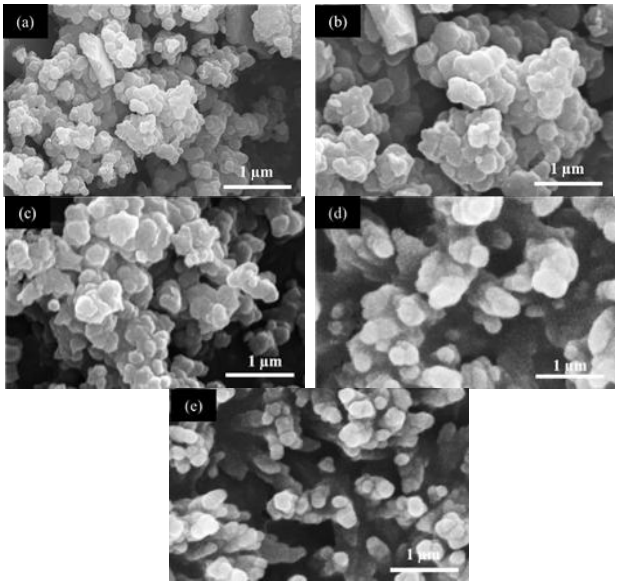

Figure 2: SEM of silica (a), composites SP1 (b), SP2 (c), SP3 (d) and SP4 (e)

Table 2: EDX data of SP1, SP2, SP3 and SP4

	C	O	N	Si
SP1	39.68	31.43	8.41	20.48
SP2	34.82	35.94	8.05	21.19
SP3	31.77	35.05	8.15	25.03
SP4	29.02	34.83	8.01	28.14

The EDX analysis of SP1, SP2, SP3 and SP4 identified the presence of C, N, O and Si, as the main constituent elements of the deposit (Figure 4). Carbon and nitrogen are the main elements in the

polypyrrole compound. The presence of silicon and oxygen is in agreement with the fact that the incorporation between PPy and SiO_2. The quantities of silica increase from SP1 to SP4 in initial mixture, the weight percentage of silicon increase to 20.48, 21.19, 25.03 and 28.14 with SP1, SP2, SP3 and SP4, respectively (table 2).

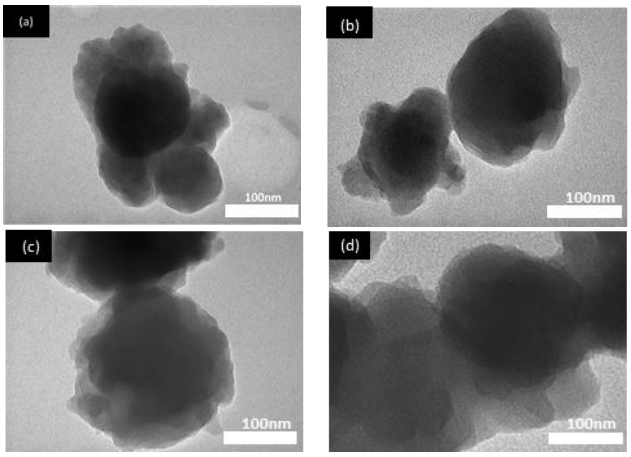

Figure 3: TEM composites SP1 (a), SP2 (b), SP3 (c) and SP4 (d)

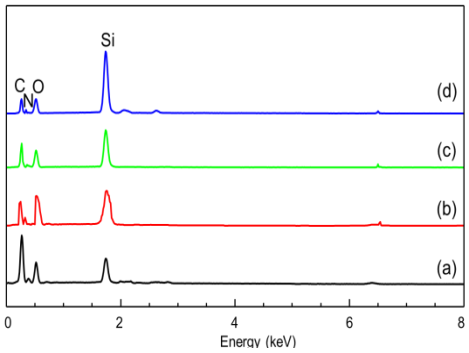

Figure 4: EDX of composites SP1 (a), SP2 (b), SP3 (c) and SP4 (d)

3.3. TGA

Figure 5 shows TGA thermograms of PPy, SP1, SP2, SP3 and SP4. With all samples, the weight loss occurs in three different stages. For pure PPy, the first weight loss starts below 120 ^oC due the elimination of absorbed water and above 220^oC corresponds to the polymer chain degradation. The amount of silica in composites SP1, SP2, SP3 and SP4 was calculated from TGA curves by comparing the amount of residue of composites with those assigned to pure PPy. For this purpose, it was assumed that PPy in the composite are the origins of an amount of residue proportional to the amount of each pure component. So the weight percentage of silica in SP1, SP2, SP3 and SP4 are 28, 36, 39 and 48 %.

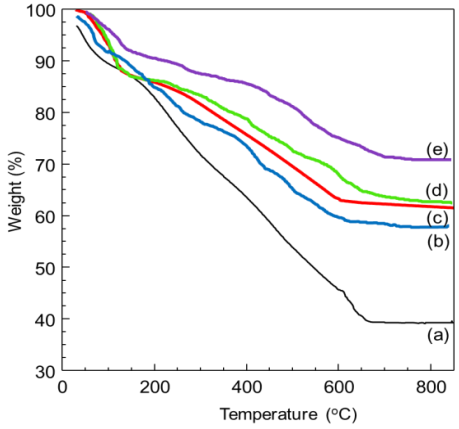

Figure 5: TGA diagram of PPy (a), composites SP1 (b), SP2 (c), SP3 (d) and SP4 (e)

3.4. Open circuit potential

Figure 6 presents open circuit curves of steel coated with PVB and PVB containing 10 % SP1, SP2, SP3 and SP4 after 48 hours immersion in 3 % NaCl solution. At the beginning, the potential of steel coated with PVB is -0.34 V_{SCE} and decrease continuous to -0.69 V_{SCE} after 48 hours. In the beginning, with SP1, SP2, SP3 and SP4, the potential is -0.080, -0.075, -0.074 and -0.12 V_{SCE}, respectively. This shows that coating have exhibited effective barrier behavior and limited the motion of corrosive agent towards the underlying metal. However, trend of OCP variation of SP1, SP2, SP3 and SP4 shifted sharply after 20 hours immersion. After this, the potential is stable for about 10 hours, then towards negative potential and achieves -0.375, -0.451, -0.475 and -0.476 V_{SCE}, respectively, after 48 hours. That means composites can shift the potential of steel into anode areas, but the coatings are thin, so chloride ions diffuse rapidly through the coating to the metal surface, so the potential decreases.

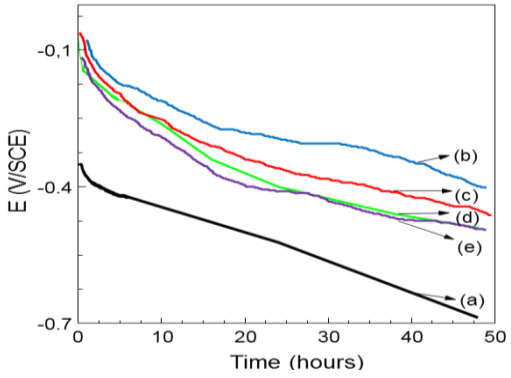

Figure 6: Open circuit potential with time of steel coated with PVB (a), PVB containing 10 % composites SP1 (b), SP2 (c), SP3 (d) and SP4 (e)

3.5. Potentiodynamic polarization

Figure 7 shows Tafel curves of steel coated with PVB and steel coated with PVB containing 10 % SP1, SP2, SP3 and SP4 in 3 % NaCl solution after 48 hours. The values of corrosion potential (E_{corr}), corrosion current density (i_{corr}), anodic and cathodic Tafel constants (β_a, β_c), polarization resistance (Rp) are given in table 3.

Corrosion potential for the steel coated with SP1, SP2, SP3 and SP4 shift to more positive regions compared with the steel coated with PVB indicates that the corrosion process is inhibited by the composites SiO_2/PPy. Analysis of the data given in Table 3 shows that i_{corr} values of steel coated with PVB containing 10 % SP1, SP2, SP3 and SP4 decrease significantly, it is two and more than two orders of magnitude less when compared to that of steel coated with PVB. Further, the occurrence of notably higher value of anodic and cathodic Tafel constants for SP1, SP2, SP3 and SP4 implies the effective role of SiO_2/PPy composites in controlling anodic and cathodic corrosion reaction. Among the protective coatings, the PVB-SP1 coating has the lowest corrosion current density (1.05×10^{-8} A.cm^{-2}) and hence the highest polarization resistance (9.1×10^{6} Ω). These results confirm that composites can improve the corrosion protection performance of coatings.

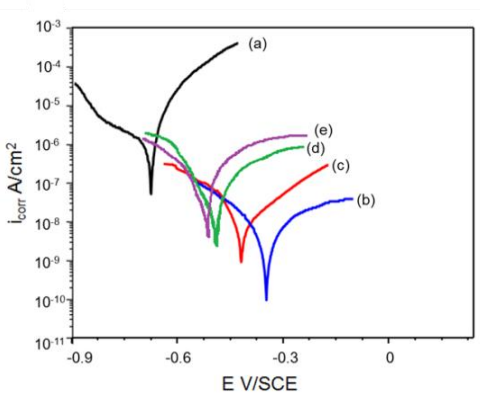

Figure 7: Polarization curves of steel coated with PVB (a), PVB containing 10 % composites SP1 (b), SP2 (c), SP3 (d) and SP4 (e) after 48 hours immersion in 3 % NaCl solution

Table 3: Electrochemical parameters obtained from Tafel extrapolation of the steel coated with PVB, PVB containing 10 % nanocomposites SP1, SP2, SP3 and SP4 after 48 hours immersion in 3 % NaCl solution

Samples	E_{corr} (V)	β_a (V dec^{-1})	β_c (V dec^{-1})	i_{corr} (A.cm^{-2})	R_p (Ω)
PVB	-0.676	0.314	0.105	2.78×10^{-6}	2.3×10^{3}
PVB-SP1	-0.362	0.774	0.307	1.05×10^{-8}	9.1×10^{6}
PVB-SP2	-0.427	0.524	0.215	2.06×10^{-8}	3.2×10^{6}
PVB-SP3	-0.509	0.319	0.121	8.34×10^{-8}	4.6×10^{5}
PVB-SP4	-0.520	0.373	0.115	7.52×10^{-8}	5.1×10^{5}

4. CONCLUSION

Composites SiO_2/PPy core shell are successfully synthesized by in-situ method. The results show that synthesized composites can improve corrosion protection performance of PVB coating for steel in 3 % NaCl solution. Composite SiO_2/PPy is promising in view as inhibitors of organic coatings.

Acknowledgements. *This research is funded by Vietnam National Foundation for Science and Technology Development (NAFOSTED) under grant number 104.06-2014.12.*

REFERENCES

1. A. G. MacDiarmid. *Short Course on Conductive Polymers*, SUNY, New Platz-NY (1985).
2. T. Ohtsuka. *Corrosion Protection of Steels by Conducting Polymer Coating*, International Journal of Corrosion (2012), http://dx.doi.org/10.1155/2012/915090
3. P. P. Deshpande, N. G. Jadhav, V. J. Gelling, D. Sazou. *Conducting polymers for corrosion protection: A review*, Journal of Coatings Technology and Research, **11(4)**, 473-494 (2014).
4. R. W. Revie, Canmet. *Corrosion HandBook*, 3rd Ed., Ottawa, Ontario, Canada (2011).
5. M. A. Hussein, S. S. Al-Juaid, B. M. Abu-Zied, A. A. Hermas. *Electrodeposition and Corrosion Protection Performance of Polypyrrole Composites on Aluminum*, International Journal of Electrochemical Science, **11**, 3938-3951 (2016).
6. N. V. Krstajíc, B. N. Grgur, S. M. Jovanovíc, M. V. Vojnovíc. *Corrosion protection of mild steel by polypyrrole coatings in acid sulfate solutions*, Electrochimica Acta, **42(11)**, 1685- 1691 (1997).
7. G. Ruhi, H. Bhandari, S. K. Dhawan. *Corrosion Resistant Polypyrrole/Flyash Composite Coatings*

Designed for Mild Steel Substrate, American Journal of Polymer Science, **5(1A)**, 18-27 (2015).
8. L. M. Duc, V. Q. Trung, INTECH, **7**, 143 (2013).
9. H. N. T. Le, B. Garcia, C. Deslouis, Q. L. Xuan. *Corrosion protection and conducting polymers: polypyrrole films on iron*, Electrochimica Acta, **46**, 4259-4272 (2001).
10. N. Su, H. B. Li, S. J. Yuan, S. P. Yi, E. Q. Yin. *Synthesis and characterization of polypyrrole doped with anionic spherical polyelectrolyte brushes*, Express Polymer Letters, **6(9)**, 697-705 (2012).
11. M. R. Mahmoudian, Y. Alias, W. J. Basirun, M. Ebadi. *Effects of different polypyrrole/TiO_2 nanocomposite morphologies in polyvinyl butyral coatings for preventing the corrosion of mild steel*, Applied Surface Science, **268**, 302-311 (2013).
12. M. R. Mahmoudian, Y. Alias, W. J. Basirun, A. K. Zak. *Electrochemical characteristics of coated steel with poly(N-methyl pyrrole) synthesized in presence of ZnO nanoparticles*, Thin solid Films, **520**, 258-265 (2011).
13. O. Zubillage, F. J. Cano, I. Azkarate, I. S. Molchan, G. E. Thompson, A. M. Cabral, P. J. Morais. *Corrosion performance of anodic films containing polyaniline and TiO_2 nanoparticles on AA3105 aluminium alloy*, Surface and Coatings Technology, **202**, 5936-5942 (2008).
14. S. P. Sitaram, J. O. Stoffer, T. J. O'Keefe. *Application of conducting polymers in corrosion protection*, Journal of Coatings Technology, **69(866)**, 65-70 (1997).
15. H. Zou, S. Wu, J. Shen. *Polymer/silica nanocomposites: Preparation, Characterization, Properties and Applications*, Chemical Reviews, **108**, 3893-3957 (2008).
16. T. Dai, X. Yang, Y. Lu. *Conductive composites of polypyrrole and sulfonic-functionalized silica spheres*, Materials Letters, **61**, 3142-3145 (2007).
17. L. Y. Hao, C. L. Zhu, W. Q. Jiang, C. N. Chen, Y. Hub, Z. Y. Chen. *Sandwich Fe_2O_3-SiO_2-PPy ellipsoidal spheres and four types of hollow capsules by hematite olivary particles*, Journal of Material Chemistry, **1**, 2929-2934 (2004).
18. S. Maeda, S. P. Armes. *Preparation of Novel Polypyrrole-Silica Colloidal Nanocomposites*, Journal of Colloid Interface Science, **159**, 257-259 (1993).
19. S. Maeda, S. P. Armes. *Preparation and characterisation of novel polypyrrole-silica colloidal nanocomposites*, Journal of Material Chemistry, **4**, 935-942 (1994).
20. C. Perruchot, M. M. Chehimi, M. Delamar, F. Fievet. *Use of aminosilane coupling agent in the synthesis of conducting, hybrid polypyrrole-silica gel particles*, Surface and Interface Analysis, **26(9)**, 689-698 (1998).
21. C. Perruchot, M. M. Chehimi, D. Mordenti, M. Briand, M. Delamar. *The role of a silane coupling agent in the synthesis of hybrid polypyrrole-silica gel conducting particles*, Journal of Material Chemistry, **8**, 2185-2193 (1998).
22. A. A. Farghaly, M. M. Collinson. *Mesoporous Hybrid Polypyrrole-Silica Nanocomposite Films with a Strata-Like Structure*, Langmuir, **32**, 5925-5936 (2016).
23. Q. Cheng, V. Pavlinek, A. Lengalova, C. Li, Y. He, and P. Saha. *Conducting polypyrrole confined in ordered mesoporous silica SBA-15 channels: preparation and its electrorheology*, Microporous and Mesoporous Materials, **93(1-3)**, 263-269 (2006).
24. M. Marini, F. Pilati, B. Pourabbas, Macromol. *Smooth Surface Polypyrrole-Silica Core-Shell Nanoparticles: Preparation, Characterization and Properties*, Chemical Physical, **209**, 1374-1380 (2008).
25. M. Stern, A.L. Geary. *Electrochemical Polarization: A Theoretical Analysis of the Shape of Polarization Curves*, Journal of the Electrochemical Society, **104(12)**, 751-752 (1957).
26. F. Yang, Y. Chu, S. Ma, Y. Zhang, J. Liu. *Preparation of uniform silica/polypyrrole core/shell microspheres and polypyrrole hollow microspheres by the template of modified silica particles using different modified agents*, Journal of Colloid and Interface Science, **301**, 470-478 (2006).
27. Y. Dae Kim, G. Hong. *Electrorheological properties of polypyrrole-silica nanocomposite suspensions*, Korean Journal Chemistry English, **29(7)**, 964-968 (2012).
28. X. Liu, H. Wu, F. Ren, G. Qiu, M. Tang. *Controllable fabrication of SiO_2/polypyrrole core-shell particles and polypyrrole hollow spheres*, Materials Chemistry and Physics, **109**, 5-9 (2008).
29. I. Y. Jeon, H. J. Choi, L. S. Tan, J. B. Baek. *Nanocomposite prepared from in situ grafting of polypyrrole toaminobenzoyl-functionalized multiwalled carbon nanotube and its electrochemical properties*, Journal of Polymer Science Part A: Polymer Chemistry, **49**, 2529-2537 (2011).
30. W. Su, J. O. Iroh. *Electropolymerzation of pyrrole on steel substrate in the presence of oxalic and amines*, Electrochimica Acta, **44**, 2173-2184 (1999).

Corresponding author: **Dinh Thi Mai Thanh**
Institute for Tropical Technology
Vietnam Academy of Science and Technology
18, Hoang Quoc Viet road, Cau Giay district, Hanoi, Viet Nam
E-mail: dmthanh@itt.vast.vn.